ACS OMEGA

http://pubs.acs.org/journal/acsodf

Article

Synthesis, Biological Evaluation, and *In Silico* Studies of Novel Coumarin-Based 4*H*,5*H*-pyrano[3,2-*c*]chromenes as Potent *β*-Glucuronidase and Carbonic Anhydrase Inhibitors

Nadia Arif, Zahid Shafiq,* Khalid Mahmood, Muhammad Rafiq, Sadia Naz, Sohail Anjum Shahzad, Umar Farooq, Ali H. Bahkali, Abdallah M. Elgorban, Muhammad Yaqub,* and Ahmed El-Gokha

Cite This: *ACS Omega* 2022, 7, 28605−28617

Read Online

ACCESS | Metrics & More | Article Recommendations | Supporting Information

ABSTRACT: The search for novel heterocyclic compounds with a natural product skeleton as potent enzyme inhibitors against clinical hits is our prime concern in this study. Here, a simple and facile two-step strategy has been designed to synthesize a series of novel coumarin-based dihydropyranochromenes (**12a−12m**) in a basic moiety. The synthesized compounds were thus characterized through spectroscopic techniques and screened for inhibition potency against the cytosolic hCA II isoform and *β*-glucuronidase. Few of these compounds were potent inhibitors of hCA II and *β*-glucuronidase with varying IC_{50} values ranging from 4.55 ± 0.22 to 21.77 ± 3.32 *μ*M and 440.1 ± 1.17 to 971.3 ± 0.05 *μ*M, respectively. Among the stream of synthesized compounds, **12e** and **12i** were the most potent inhibitors of *β*-glucuronidase, while **12h**, **12i**, and **12j** showed greater potency against hCA II. *In silico* docking studies illustrated the significance of substituted groups on the pyranochromene skeleton and binding pattern of these highly potent compounds inside enzyme pockets.

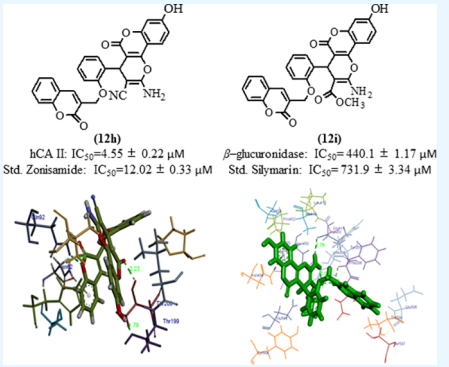

INTRODUCTION

β-Glucuronidase belongs to the family of lysosomal enzymes, which brings about the cleavage of glucuronosyl-*O*-bond, thus removing individual sugars from glycosaminoglycans (GAGs).[1] The shortage of *β*-glucuronidase in body tissues consequently results in proliferation of GAGs inside the lysosomes, leading to the enlargement of their size.[2] As a consequence of over-expression of this enzyme in various cancers like the neoplasm of bladder,[3] liver cancer,[4] and colon carcinoma,[5,6] the quantitative measurement of *β*-glucuronidase has been proved as a detection tool at the initial stage diagnosis of cancer and the assessment of therapeutic treatments.[7,8] Moreover, it is evident from the literature that an elevated level of *β*-glucuronidase in blood serum is related to various physiological disorders such as urinary tract infection,[9] rejection of transplantation,[10] epilepsy,[11] renal diseases,[12] rheumatoid arthritis,[13] and larynx[14] and breast cancer.[15] Besides these, acquired immune deficiency syndrome (AIDs) and hepatic disorders have also been reported as a consequence of a high level of this enzyme.[16,17]

Carbonic anhydrase (CA) isoenzymes are pervasive members of metalloenzymes with a Zn(II) ion metallic core at the active center of the enzyme.[18,19] They are prevalent in all organisms where they are engaged in the reversible catalysis of hydration of CO_2 to (HCO_3^{-1}) and (H^+).[20] This reaction is associated with various physiological processes in humans such as electrolytic secretion, pH regulation, gluconeogenesis, lipogenesis, bone resorption, calcification, tumorigenicity, and various other pathological processes.[21] CAs are committed as attractive targets for drug design to cure therapeutic diseases like acid−base disequilibria, epilepsy, glaucoma, cancer, osteoporosis and other neuromuscular disorders, edema, altitude sickness, and obesity.[22,23] Recent studies have shown the role of CA inhibitors (CAIs) as a therapeutic hit for other diseases like neuropathic pain,[24] cerebral ischemia,[25] and tumor.[26] The unexpected and novel application of CAIs in synaptic transformation and attentional gating of memory is quite appreciating in the treatment of Alzheimer's disease.[27]

The synthesis of efficient heterocyclic molecules with a natural product core and their exploration as therapeutic agents against human diseases have become an indispensable paradigm of clinical trials in modern drug development.[28] Chromenes and coumarins[29] are among the O-ring heterocycles with a benzopyrone skeleton and have gained the attention of pharmaceutical chemists for a number of years because of their therapeutic potential and biological significance.[30,31] The ubiquitous chromene framework is well known for several pharmacological activities like antifungal,[32]

Received: June 6, 2022
Accepted: July 26, 2022
Published: August 4, 2022

https://doi.org/10.1021/acsomega.2c03528
ACS Omega 2022, 7, 28605−28617

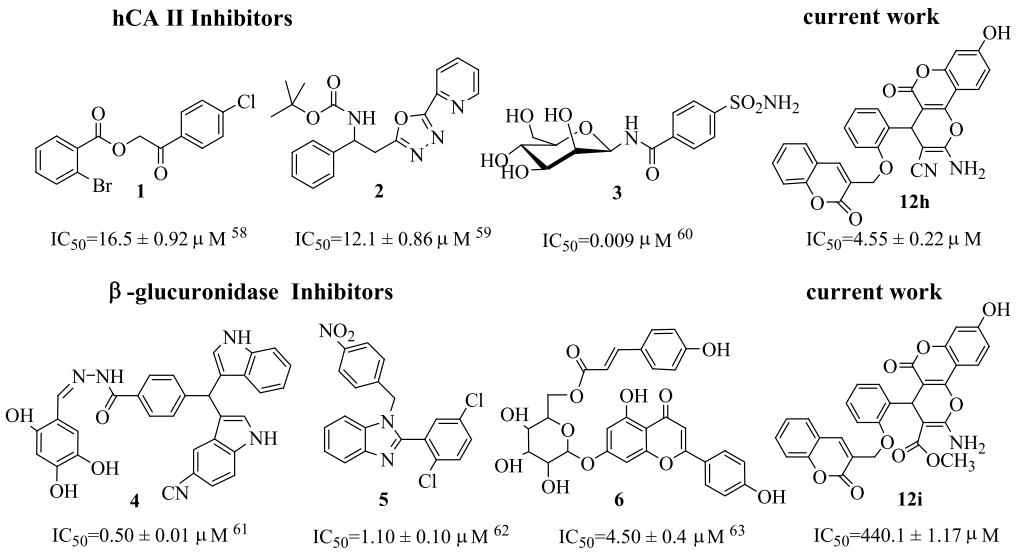

Figure 1. Selected hCA II/β-glucuronidase inhibitors and current work.

Scheme 1. Synthesis of Coumarin-Based 4*H*,5*H*-Pyrano[3,2-*c*]chromenes (12a−12m)

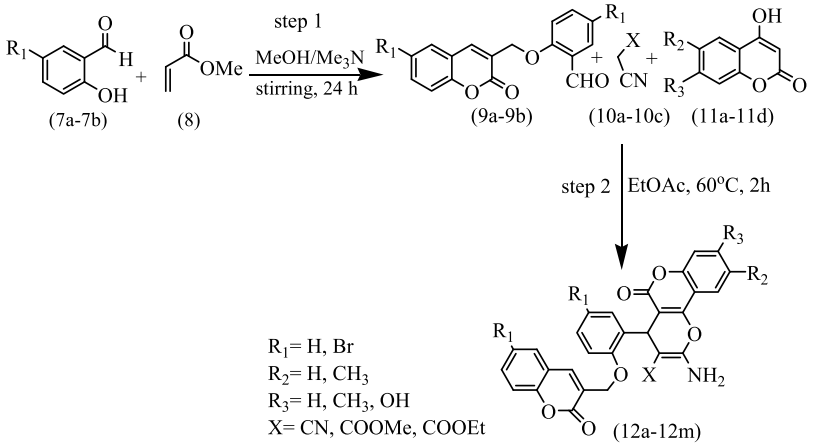

antimicrobial,[33] antiviral,[34] anti-allergic,[35] antiulcer,[36] and anti-inflammatory activities.[37] Furthermore, fused-chromene compounds are renowned to exhibit a wide range of therapeutic applications starting with antitumor,[38] antileishmanial,[39] antiproliferation,[40] anti-HIV agent,[41] and antioxidative applications.[42] The substituted side chains in the structural framework of benzopyran exhibited the pharmaceutical potential of coumarin-containing drugs, thus exploring their prominence in synthetic and clinical perspective.[43]

Coumarin-based compounds are reported as a class of CAIs possessing unique features of their skeletal structure for binding with carbonic anhydrase enzyme.[44] Some of the first- and second-generation pharmacophores like sulfamides, sulfamates, and sulfonamides, still utilized in medical treatment as CAIs, are zinc binders exhibiting various complications.[45−48] Contrary to the above-mentioned compounds, coumarins and thiocoumarins are contrived as CAIs[49] for selective inhibition of hCA isoforms, exploring an inhibition pathway not vulnerable to Zn^{2+} (Figure S1).[50,51] Coumarin compounds are hydrolyzed by the esterase activity of CA and proposed to bind with the entrance of the active site of hCA, the region that is quite variable in various isoforms, where the interaction of coumarin substrates with amino acids leads to higher selectivity toward various isoforms.[52,53] Earlier studies from the literature revealed that some of the coumarin derivatives could not access the enzyme cavity of CA due to bulkiness, which therefore could not be hydrolyzed by the esterase activity of the enzyme.[54−57]

Some of the selected compounds from the literature[58−63] are reported here in Figure 1 as hCA II and β-glucuronidase inhibitors, which are rationalized with current work to disclose their metabolic liabilities and/or biological potencies.

Encouraged by above findings about coumarins and chromenes in enzyme inhibition and their role in drug development, we have decided to employ this privileged core with multifarious medicinal properties in synthesizing a series of novel fused ring dihydropyranochromenes (**12a−12m**). Furthermore, these synthesized compounds were subjected to enzyme inhibition studies to find new inhibitors. β-Glucuronidase and carbonic anhydrase are among the important enzyme targets discussed in the present study for inhibitory properties of synthesized biomolecules against the diseased state. The molecular docking[64−68] study of synthesized compounds is also reported here to compare the results of biological potential of molecules with theoretical calculations.

https://doi.org/10.1021/acsomega.2c03528
ACS Omega 2022, 7, 28605−28617

RESULTS AND DISCUSSION

Chemistry. In our targeted approach toward seeking O-ring heterocycles (chromenes) as potent enzyme inhibitors, a series of novel fused ring coumarin-based dihydropyranochromenes (**12a−12m**) were synthesized in two steps (Scheme 1). In the first step, coumarin-based aldehydes (**9a−9b**) were synthesized by utilizing the Baylis−Hillman reaction protocol as depicted in the literature.[69] Compound **9a** showed physical parameters (i.e., color, m.p., etc.) and spectroscopic data precisely unified with literature values.[69] The structure of the other novel bromo-substituted coumarin-based aldehyde (**9b**) was precisely verified from its spectroscopic data that was in good agreement. The presence of aldehydic and ester moieties in these precursors could be easily depicted on the basis of IR stretching frequency bands in the regions of 1670−1695 and 1700−1730 cm^{-1}, and the ^1H NMR spectra also unveiled the singlet of 1H at δ 10.48−10.53 ppm for the presence of a CHO group. The ^{13}C NMR spectra of compound **9a** also displayed required chemical shifts, i.e., δ 125−150 ppm (aromatic region) and δ 190.17 ppm (aldehydic-C). The collected experimental data from elemental analysis was also in close agreement with calculated % ages of elements in targeted heterocyclic compounds. In the second step (Scheme 1), arylidenes of respective aldehydes (**9a** and **9b**) with different nitriles (**10a−10c**) were further treated with different derivatives of 4-hydroxycoumarin (**11a−11d**) in the presence of Et_3N through the Knoevenagel−Michael cyclization path in a one-pot strategy to get targeted dihydropyranochromenes (**12a−12m**) with excellent yield (Table 1). The enhancement in the regioselectivity of reaction as well as yield of product was obtained by monitoring various parameters during the course of reaction (i.e., temperature, solvent, and catalyst). The optimization of various reaction parameters for the preparation of model compound **12a** is illustrated in Table S1. Thus, ethyl acetate as a solvent, Et_3N or Me_3N as a base, and 60 °C temperature were found to be the suitable parameters for this reaction. Spectroscopic techniques like IR, NMR, etc., were utilized to elaborate the structure of a synthesized series of targeted heterocycles. The absorption peaks in the ranges of 1680−1735 and 2190−2197 cm^{-1} and two peaks at 3150−3300 and 3300−3450 cm^{-1} were used to identify the desired functionalities like carbonyl, cyano, and NH_2 groups in the relevant product. The evidence for other substituents such as the OH group on the coumarin skeleton was also comprehended on the basis of the absorption band at 3400−3650 cm^{-1}. The ^1H NMR spectra of **12a−12m** gave the confirmation of cyclized products as there was no downfield signal of CHO proton at δ 10.48−10.53 ppm; instead, a singlet of two protons for the NH_2 group was observed at δ 7.10−7.70 ppm, and this peak was merged in the aromatic range in accordance with shielding or deshielding. Further evidence for the cyclized product came from the fact that the signal for a singlet of the OH group of 4-hydroxylated coumarins disappeared as well. The appearance of two signals (i.e., triplet of 3H at δ 0.80−1.10 ppm and quartet of 2H at δ 3.95−3.96 ppm) and one signal for the singlet of 3H at δ 3.50−3.52 ppm illustrated the ethyl ester in **12c**, **12f**, **12g**, and **12j** and methyl-ester in compounds **12b**, **12e**, and **12i**, respectively. Total proton counts in the aromatic region also fulfill the structural requirement of the compound. Their chemical shifts were allocated on behalf of spin multiplicity as well as coupling constant. The ^{13}C NMR spectra of **12a−12m** unveiled the accordance of chemical shifts of aliphatic, aromatic, and carbonyl moieties with desired structures. Further confirmation of representative compound **12a** came from absorption peaks of aliphatic carbons at 32.63 and 57.25 ppm, aromatic carbons at 125−150 ppm, and carbonyl at 159.88 and 160.4 ppm. CHN analyses satisfactorily supported the desired structure of targeted dihydropyranochromenes, as experimentally collected data was in close agreement with calculated % ages.

Table 1. Coumarin-Based 4*H*,5*H*-Pyrano[3,2-*c*]chromenes (12a−12m)

compound no.	R_1	R_2	R_3	X	% age yield
12a	H	H	H	CN	97
12b	H	H	H	$COOCH_3$	95
12c	H	H	H	$COOC_2H_5$	95
12d	H	CH_3	H	CN	96
12e	H	CH_3	H	$COOCH_3$	90
12f	H	CH_3	H	$COOC_2H_5$	92
12g	H	H	CH_3	$COOC_2H_5$	94
12h	H	H	OH	CN	94
12i	H	H	OH	$COOCH_3$	70
12j	H	H	OH	$COOC_2H_5$	74
12k	Br	H	H	CN	52
12l	Br	CH_3	H	CN	52
12m	Br	H	CH_3	CN	48

Biological Evaluation. *In Vitro hCA II Inhibition.* Literature findings enlighten the scope of CA inhibition study in the clinical treatment of various therapeutic diseases like acid−base disequilibria, cancer, epilepsy, glaucoma, osteoporosis and neuromuscular disorders, edema, altitude sickness, obesity, etc.[22,23] In this perspective, the role of coumarin-based compounds as CAIs cannot be ignored.[44] In the present study, a series of synthesized compounds (**12a−12m**) were tested against cytosolic hCA II. The inhibition results of the stream of synthesized compounds are presented in Table 2a, which explore the broad spectrum of inhibitory potential against cytosolic hCA II using zonisamide as a reference. IC_{50} values thus obtained were found to be staggered between 4.55 ± 0.22 and 21.77 ± 3.32 μM. Few of these compounds like **12h**, **12i**, and **12j** with IC_{50} = 4.55 ± 0.22, 4.91 ± 1.13, and 7.78 ± 0.08 μM, respectively, unveiled excellent inhibitory power to block the enzyme. An innovative

Table 2a. Inhibitory Activity of Compounds 12a−12m against hCA II

compound no.	IC_{50} (μM ± SEM)
12a	
12b	
12c	
12d	
12e	21.77 ± 3.32
12f	
12g	
12h	4.55 ± 0.22
12i	4.91 ± 1.13
12j	7.78 ± 0.08
12k	
12l	
12m	
zonisamide (std.)	12.02 ± 0.33

https://doi.org/10.1021/acsomega.2c03528
ACS Omega 2022, 7, 28605−28617

inhibition mechanism has been proposed based on the activity profile of the series of synthesized coumarin derivatives. Our reported compounds in this study could not enter deep inside the cavity of the enzyme due to their massive size, therefore attaching at the mouth of the cavity of hCA II via substituents present at the phenyl ring of the coumarin skeleton. This inhibition mode followed by these coumarin derivatives because of their bulkiness is called the allosteric inhibition pathway. Thus, the high-rank inhibitory potential of compounds **12h**, **12i**, and **12j** against hCA II is attributed to the presence of the electron-donating OH group at C-7 of the coumarin motif. Compound **12e** also exhibits moderate inhibitory power, bearing a CH_3 group at C-6 of coumarin and $COOCH_3$ and NH_2 on the pyran ring. Compounds **12a**−**12m** showed the following descending order of inhibitory activity illustrated on behalf of the SAR study of compounds: **12h** > **12i** > **12j** > **12e**.

In Vitro β-Glucuronidase Inhibition. Owing to the great therapeutic potential of synthetic coumarins as enzyme inhibitory molecules and important drug candidates,[30,31,43] the prepared coumarin-based pyranochromenes captivated our attention to bring about this study. Thus, the β-glucuronidase inhibitory power of synthesized derivatives (**12a**−**12m**) was checked by utilizing the literature protocol[74] and IC_{50} values calculated were compared with std. silymarin. The results are illustrated in Table 2b, which showed inhibition of IC_{50} ± SEM in the range from 440.1 ± 1.17 to 971.3 ± 0.05 μM. Compounds **12e** with IC_{50} = 670.7 ± 1.18 μM and **12i** with IC_{50} = 440.1 ± 1.17 μM were found to be more active against this enzyme when compared with std. silymarin with IC_{50} = 731.9 ± 3.34 μM, while other compounds with mild inhibitory power are **12d** (IC_{50} = 789.5 ± 0.75 μM), **12g** (IC_{50} = 971.3 ± 0.05 μM), and **12j** (IC_{50} = 773.9 ± 2.22 μM). The SAR studies on these *O*-heterocycles reveal that the presence of the $COOCH_3$ group on the pyran ring of **12e** and **12i** may be responsible for this high-rank inhibitory potential against β-glucuronidase. Furthermore, the presence of the electron-donating OH group at C-7 of the coumarin nucleus enhanced the activity in compound **12i**. Compounds **12a**−**12m** showed the following descending order of inhibitory activity illustrated on behalf of the SAR study of compounds: **12i** > **12e** > **12j** > **12d** > **12g**.

Table 2b. Inhibitory Activity of Compounds 12a−12m against β-Glucuronidase

compound no.	IC_{50} (μM ± SEM)
12a	
12b	
12c	
12d	789.5 ± 0.75
12e	670.7 ± 1.18
12f	
12g	971.3 ± 0.05
12h	
12i	440.1 ± 1.17
12j	773.9 ± 2.22
12k	
12l	
12m	
silymarin (std.)	731.9 ± 3.34

Molecular Docking Studies. Molecular docking studies enabled scientists in recent decades to unveil the interaction and binding tendency of a given molecule inside the active pocket of protein. The use of molecular docking studies to rationalize the mechanism behind various fundamental biochemical processes is well documented.[70−72] Keeping in view the good enzyme inhibitory potential of synthesized compounds **12a**−**12m**, we performed molecular docking studies against carbonic anhydrase II and β-glucoronidase enzyme. The compounds having a good binding score presented in Tables 3a and 3b and an interaction pattern inside the active pocket of given enzymes gave insight into their inhibitory potential and suggested them as potent inhibitors. The binding interaction of potent inhibitors with active site residues of hCA II and β-glucoronidase is mentioned in Table S2.

Table 3a. Binding Scores and RMSD Values of Compounds 12a−12m against hCA II[a]

compound	binding score (kcal/mol)	RMSD
12a	−1.439	0.9582
12b	−1.595	0.6821
12c	1.017	1.0012
12d	1.265	0.8983
12e	−4.265	0.8790
12f	−1.688	0.9951
12g	−1.022	0.9937
12h	−13.627	0.5491
12i	−11.252	0.8540
12j	−9.886	0.8213
12k	1.256	1.2213
12l	1.024	1.0326
12m	1.289	1.2241
zonisamide	−2.873	0.8859

[a]RMSD: RMSD of the docking pose compared to the cocrystal ligand position; "−" represents a positive or bad binding score.

Table 3b. Binding Scores and RMSD Values of Compounds 12a−12m against β-Glucuronidase[a]

compound	binding score (kcal/mol)	RMSD
12a	−1.892	1.0481
12b	−2.339	0.8791
12c	−1.492	0.8849
12d	−5.581	0.9396
12e	−6.749	0.9030
12f	−1.238	1.0281
12g	−4.319	1.1043
12h	−2.994	1.0130
12i	−7.894	0.8769
12j	−5.827	0.7919
12k	−2.987	0.9901
12l	−1.485	0.9926
12m	−2.473	0.9859
silymarin (std.)	−4.984	0.9683

[a]RMSD: RMSD of the docking pose compared to the cocrystal ligand position; "−" represents a positive or bad binding score.

Carbonic Anhydrase II. On account of results obtained from *in vitro* CA II studies, compounds **12h**, **12i**, and **12j** exhibited potent inhibition against the hCA II isoform. Thus, the inhibition mechanism of these highly potent compounds

https://doi.org/10.1021/acsomega.2c03528
ACS Omega 2022, 7, 28605−28617

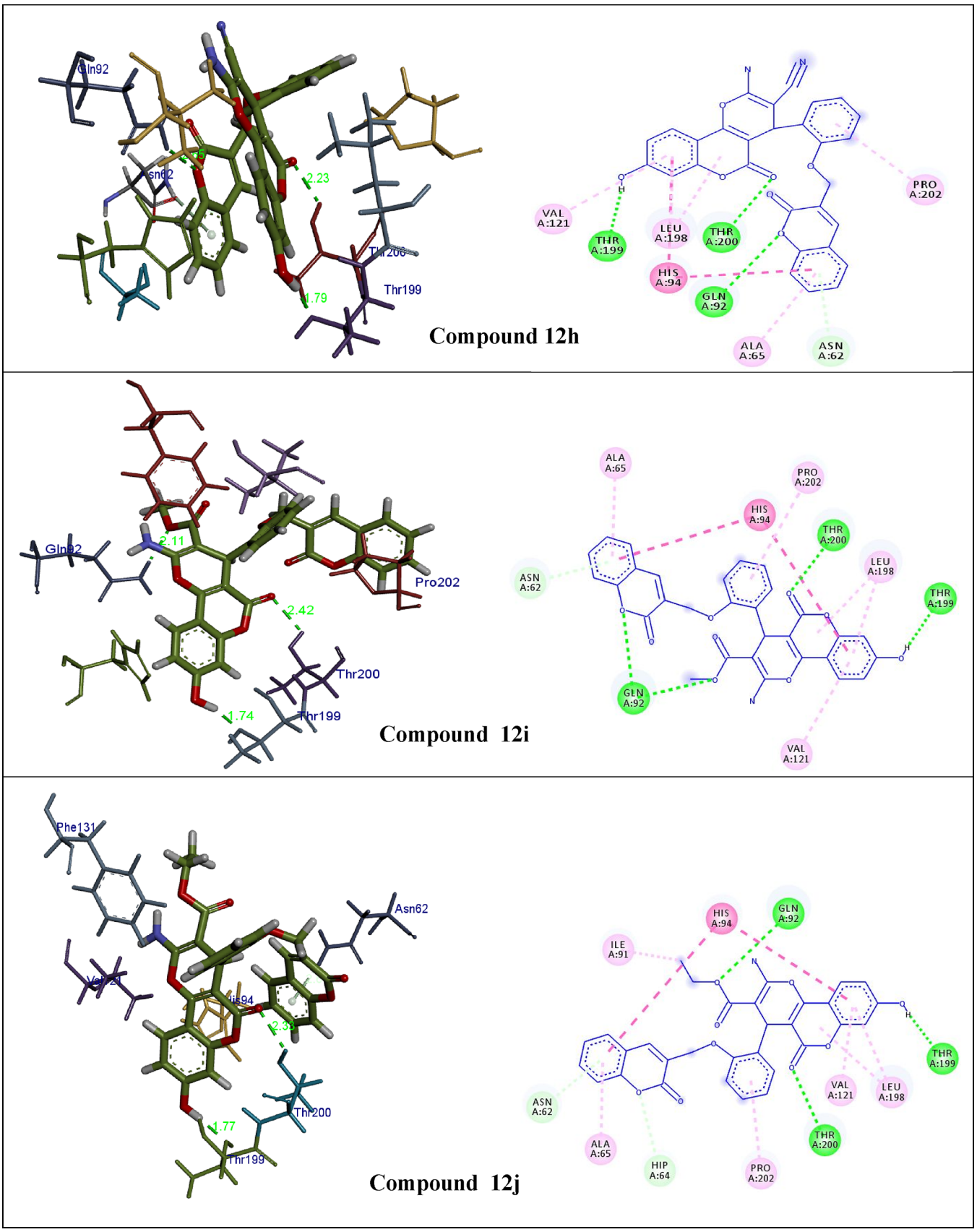

Figure 2. 3D and 2D views of the binding interaction pattern of compounds **12h**, **12i**, and **12j** with active site residues of human carbonic anhydrase II (hCA II).

https://doi.org/10.1021/acsomega.2c03528
ACS Omega 2022, 7, 28605−28617

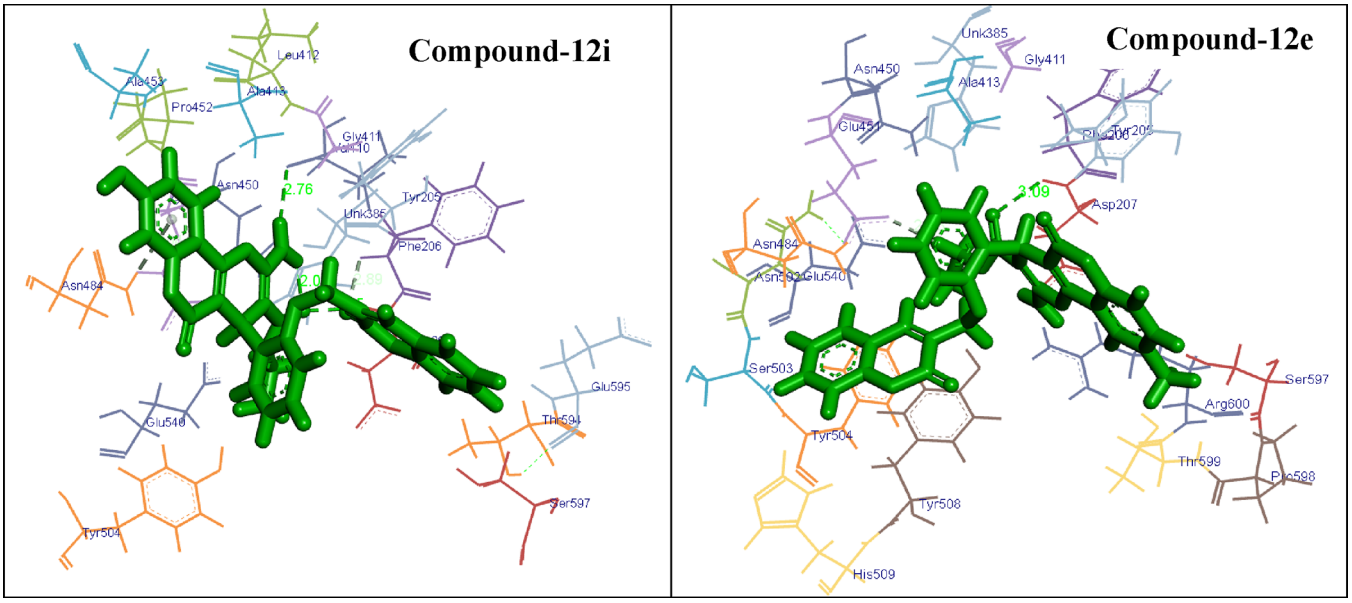

Figure 3. Binding interaction pattern of compounds **12e** and **12i** with active site residues of β-glucoronidase.

has been evaluated via molecular docking studies. The accuracy of the docking methodology was further tested with redocking phenomena, and RMSD values were evaluated and compared with docking scores. The best docked conformation was observed for compounds **12h**, **12i**, and **12j** having binding scores of −13.627, −11.252, and −9.886 kcal/mol, respectively. The molecular docking studies are facilitated to understand the mechanism behind the selective potency and inhibition tendency of these three compounds against hCA II. Previously reported coumarin derivatives as hCA II inhibitors revealed the interaction of substituents with active site residues and non-involvement of the coumarin ring due to steric hindrance,[54−57] thus exhibiting an innovative mechanistic approach where the coumarin ring could not enter deep into the active pocket of the enzyme due to bulkiness and rigidity, which therefore could not be hydrolyzed due to the esterase activity of CA II. The attachment of the molecule at the entrance of the cavity of the enzyme blocks and deshapes the active site, so the natural substrate could not enter into the enzyme pocket. This inhibition mode is illustrated as allosteric inhibition. For compound **12h**, the OH group at 7-position showed H-bonding interaction with Thr199 (1.79 Å) alongside pi−alkyl interaction with Val121 and the coumarin ring did not form any H-bonded interaction with active site residues. Similar interaction patterns were observed in the case of **12j** where coumarin rings did not interact through H-bond and the only H-bond observed was between the OH functional group and Thr199 (1.77 Å), although pi−pi stacking was revealed with His94 as shown in Figure 2. Steric hindrance prevents the coumarin ring from entering deep into the active pocket and interacting with residues. The inhibition activity of these selective compounds is attributed to allosteric inhibition due to substituents attached at the phenyl ring of coumarin rings. In the case of **12i**, we observed two H-bonding interactions with Thr199 and Gln92 alongside some pi−pi stacking and pi−alkyl interactions as depicted in Figure 2. The 2D interaction tool of Discovery Studio Visualizer was used for clear depiction of binding interactions of all these compounds inside the active pocket of hCA II (Figure 2).

β-Glucoronidase Enzyme. The compounds of current series were also evaluated through molecular docking studies for their binding tendency inside the active pocket of the β-glucoronidase enzyme. The best docked conformation was observed for compound **12i** with a binding score of −7.894 kcal/mol showing H-bonding interactions with Val410 (2.76 Å) and Asp207 (2.65 Å) alongside pi−alkyl interaction with Ala413 as shown in Figure 3. The second best binding score (−6.749 kcal/mol) was observed for compound **12e** having H-bonding interaction with Asp207 (3.09 Å), pi−pi stacking with Tyr508, and pi−anion interaction with Glu451.

2D views for the binding interaction pattern of compounds **12e** and **12i** with active site residues of β-glucoronidase are shown in Figure S1. *In silico* studies are in good agreement with *in vitro* enzyme inhibition studies and suggest some of the compounds of current series as potential inhibitors of carbonic anhydrase II and β-glucoronidase, evident from their binding scores, IC_{50} values, and binding interaction pattern inside the active pocket.

CONCLUSIONS

A series of novel coumarin-based 4*H*,5*H*-pyrano[3,2-*c*]-chromenes (**12a−12m**) were synthesized via a two-step simple, facile route and evaluated for their inhibition potency against hCA II and β-glucuronidase. Few of these compounds like **12h**, **12i**, and **12j** with IC_{50} = 4.55 ± 0.22, 4.91 ± 1.13, and 7.78 ± 0.08 μM, respectively, unveiled excellent inhibitory power against hCA II as compared to the reference compound zonisamide (IC_{50} = 12.02 ± 0.33 μM). Compounds **12e** (IC_{50} = 670.7 ± 1.18 μM) and **12i** (IC_{50} = 440.1 ± 1.17 μM) are found to be more potent against β-glucuronidase when compared with std. silymarin (IC_{50} = 731.9 ± 3.34 μM). The results from molecular docking studies showed good agreement between theoretical and experimental findings. In the future, our results would help find new CA and β-glucuronidase inhibitors and pave the direction in designing new drugs for the treatment of multifactorial clinical hits including cancer, epilepsy, Alzheimer's disease, glaucoma, and obesity.

https://doi.org/10.1021/acsomega.2c03528
ACS Omega 2022, 7, 28605−28617

EXPERIMENTAL SECTION

General Information. The required chemicals in synthetic work were purchased from a supplier and redistilled or recrystallized on need. The melting points of synthesized compounds were measured using a Fisher-Johns melting point apparatus (48061, Cole-Parmer). The reaction processing and product purity were examined utilizing TLC plates coated with Merck silica gel 60 F_{254}, while spots were envisioned in UV light (λ = 254 and 366 nm). The IR absorption spectra were taken on an FTIR instrument, while the ^{1}H NMR and ^{13}C NMR spectra of final products were done in deuterated $(CH_3)_2SO$ utilizing $(CH_3)_4Si$ as ref. std. at 300 and 400 MHz, respectively, on a Bruker AV-500 (Bruker, Rheinstetten, Forchheim, Germany). Elemental (N, C, and H) analysis was accomplished on a Leco-CHNS-9320, and results collected were in good agreement with those of calculated ones.

Synthesis. *Step 1: General Protocol for the Synthesis of Coumarin-Based Aromatic Aldehydes (**9a** and **9b**).* A standard literature methodology[69] with little amendment was adapted to prepare coumarin-based aldehydes (**9a** and **9b**). An equimolar mixture of appropriate salicylaldehyde (**7a** and **7b**) and triethylamine (5 mmol each) was stirred with methyl-acrylate (**8**) (15 mmol) in methanol or ethylacetate (5 mL) at room temperature. White precipitates appeared after 24 h of stirring, which were filtered and purified by subsequent washing and recrystallization from hot ethanol or ethylacetate. Compound **9b** was recrystallized from hot chloroform.

*Step 2: General Methodology for the Synthesis of Coumarin-Based Heterocycles (**12a**–**12m**).* An equimolar mixture of coumarin-based aldehyde (**9a** and **9b**) (1 mmol) and appropriate nitrile (**10a**–**10c**) (1 mmol) in EtOAc was initially stirred for half an hour at room temperature by employing two to three drops of Et_3N as a catalyst, and then 4-hydroxy coumarin or its substituted analog (**11a**–**11d**) (1 mmol) was added. The consumption of reactants was explored by TLC. White precipitates appeared during the course of reaction; otherwise, on cooling the reaction mixture to environmental parameters, they were filtered and washed two to three times with hot ethylacetate. Further purification was done by recrystallization using a mixture of $CHCl_3$ (4 parts) and MeOH (1 part) to furnish a pure, newly synthesized series of heterocyclic coumarin-based compounds (**12a**–**12m**) with excellent yield.

Physical and spectroscopically analyzed data of compounds **9a**, **9b**, and **12a**–**12m** is provided below.

*2-(2-Oxo-2H-chromen-3-ylmethoxy)-benzaldehyde (**9a**).* White solid; m.p. 184–186 °C; lit.[69] m.p. 190 °C; yield: 85%; solubility: $CHCl_3$, DMSO; IR, KBr (cm^{-1}): 1690, 1730; ^{1}H NMR (400 MHz, DMSO-d_6, δ, ppm): 5.15 (s, 2H, CH_2-H), 7.14 (t, 1H; J = 6.0 Hz, 11.9 Hz, Ar-H), 7.36 (d, 1H; J = 6.5 Hz, Ar-H), 7.39 (dd, 1H; J = 0.8 Hz, 6 Hz, Ar-H), 7.45 (d, 1H; J = 6.6 Hz, Ar-H), 7.63 (td, 1H; J = 5.9 Hz, 12.5 Hz; Ar-H), 7.68 (td, 1H; J = 5.8 Hz, 12.5 Hz, Ar-H), 7.76 (dd, 1H; J = 1.4 Hz, 6.1 Hz; Ar-H), 7.82 (dd, 1H, J = 1.2 Hz, 6.1 Hz, Ar-H), 7.83 (dd, 1H, J = 1.2 Hz, 6.1 Hz, Ar-H), 10.53 (s, 1H, HC=O); ^{13}C NMR (400 MHz, DMSO-d_6, δ, ppm): 66.15, 114.54, 116.59, 119.33, 121.84, 124.03, 125.20, 125.33, 128.40, 129.15, 132.35, 136.94, 140.50, 153.31, 160.05, 160.61, 190.17; anal. calcd for $C_{17}H_{12}O_4$ (280.07): C = 72.85, H = 4.32; found (%): C = 72.92, H = 4.29.

*5-Bromo-2-(6-bromo-2-oxo-2H-chromen-3-ylmethoxy)-benzaldehyde (**9b**).* White solid; m.p. 256–258 °C; yield: 85%; solubility: DMSO; IR; KBr (cm^{-1}): 1673, 1721; ^{1}H NMR (400 MHz, DMSO-d_6, δ, ppm): 5.16 (s, 2H, CH_2-H), 07.37 (d, 1H, J = 10.0 Hz; Ar-H), 07.44 (d, 1H, J = 8.8 Hz; Ar-H), 7.75–7.87 (m, 3H; Ar-H), 8.11 (s, 1H; Ar-H), 8.22 (s, 1H; Ar-H), 10.48 (s, 1H, HC=O); anal. calcd for $C_{17}H_{10}Br_2O_4$ (438.07): C = 46.61, H = 2.30; found (%): C = 46.70, H = 2.28.

*2-Amino-5-oxo-4-[2-(2-oxo-2H-chromen-3-ylmethoxy)-phenyl]-4H,5H-pyrano[3,2-c]chromene-3-carbonitrile (**12a**).* White amorphous solid; m.p. 278–280 °C; yield: 97%; solubility: DMSO; IR, KBr (cm^{-1}): 1695, 1741 (−carbonyl), 2198 (−CN), 3315, 3430 (NH_2-str.); ^{1}H NMR (400 MHz, DMSO-d_6, δ, ppm): 4.74 (s, 1H, CH, C_4-H), 4.54 (d, 1H, J = 10.5 Hz, CH_2-H_a), 4.96 (d, 1H, J = 10.5 Hz, CH_2-H_b), 6.94 (td, 1H, J = 0.7 Hz, 6.0 Hz, Ar-H), 7.08 (d, 1H, J = 6.5 Hz, Ar-H), 7.14 (t, 1H, J = 6.0 Hz, Ar-H), 7.20–7.26 (m, 4H, Ar-H), 7.34–7.41 (m, 3H, NH_2-H, Ar-H), 7.51 (d, 1H, J = 6.2 Hz, Ar-H), 7.54 (d, 1H, J = 6.2 Hz, Ar-H), 7.58–7.64 (m, 2H, Ar-H), 7.94 (s, 1H, CH, C_4''-H); ^{13}C NMR (400 MHz, DMSO-d_6, δ, ppm): 32.63, 57.25, 65.33, 103.76, 113.12, 113.26, 116.63, 116.82, 119.11, 120.02, 121.53, 122.36, 124.07, 124.72, 125.00, 128.93, 129.11, 130.57, 131.12, 132.27, 133.01, 141.22, 152.42, 153.42, 154.23, 156.35, 158.81, 159.88, 160.14; anal. calcd for $C_{29}H_{18}O_6N_2$ (490): C = 71.02, H = 3.70, N = 5.71; found (%): C = 71.00, H = 3.73, N = 5.68.

*2-Amino-5-oxo-4-[2-(2-oxo-2H-chromen-3-ylmethoxy)-phenyl]-4H,5H-pyrano[3,2-c]chromene-3-carboxylic Acid Methyl Ester (**12b**).* White crystalline solid; m.p. 256–258 °C; yield: 95%; solubility: DMSO, $CHCl_3$; IR, KBr (cm^{-1}): 1689, 1719 (—C=O), 3293, 3410 (NH_2-str.); ^{1}H NMR (300 MHz, DMSO-d_6, δ, ppm): 3.52 (s, 3H, COOMe-CH_3-H), 4.75 (d, 1H, J = 12.9 Hz, OCH_2-H_a), 4.80 (s, 1H, CH, C_4-H), 4.85 (d, 1H, J = 12.9 Hz, OCH_2-H_b), 6.89 (t, 1H, J = 7.2 Hz, Ar-H), 6.98 (d, 1H, J = 8.1 Hz, Ar-H), 7.08 (td, 1H, J = 1.2 Hz, 8.4 Hz, Ar-H), 7.16 (td, 1H, J = 1.5 Hz, 8.7 Hz, Ar-H), 7.29 (dd, 1H, J = 1.5 Hz, 7.5 Hz, Ar-H), 7.34–7.40 (m, 3H, Ar-H), 7.43–7.48 (m, 2H, Ar-H), 7.54–7.64 (m, 2H, Ar-H), 7.67 (s, 2H, NH_2), 7.77 (s, 1H, CH, C_4''-H); ^{13}C NMR (300 MHz, DMSO-d_6, δ, ppm): 33.78, 50.97, 65.26, 75.87, 105.29, 112.92, 113.42, 116.66, 116.72, 119.13, 120.73, 122.37, 124.20, 124.55, 125.01, 128.45, 128.92, 131.66, 132.30, 132.47, 132.71, 141.48, 152.37, 153.52, 153.95, 156.83, 159.36, 159.93, 160.39, 168.73; anal. calcd for $C_{30}H_{21}O_8N$ (523.13): C = 68.83, H = 4.04, N = 2.68; found (%): C = 68.80, H = 4.09, N = 2.70.

*2-Amino-5-oxo-4-[2-(2-oxo-2H-chromen-3-ylmethoxy)-phenyl]-4H,5H-pyrano[3,2-c]chromene-3-carboxylic Acid Ethyl Ester (**12c**).* White crystalline solid; m.p. 260–262 °C; yield: 95%; solubility: DMSO, $CHCl_3$; IR, KBr (cm^{-1}): 1688, 1716 (>C=O), 3298, 3410 (NH_2-str.); ^{1}H NMR (400 MHz, DMSO-d_6, δ, ppm): 1.10 (t, 3H, J = 6.8 Hz, COOEt-CH_3-H), 3.96 (q, 2H, COOEt-CH_2-H), 4.76 (d, 1H, J = 12.8 Hz, OCH_2-H_a), 4.81 (s, 1H, CH, C_4-H), 4.86 (d, 1H, J = 12.8 Hz, OCH_2-H_b), 6.89 (t, 1H, J = 7.3 Hz, Ar-H), 6.98 (d, 1H, J = 8.1 Hz, Ar-H), 7.08 (t, 1H, J = 7.4 Hz, Ar-H), 7.16 (td, 1H, J = 1.4 Hz, 8.7 Hz, Ar-H), 7.30 (dd, 1H, J = 1.3 Hz, 7.4 Hz, Ar-H), 7.35–7.40 (m, 3H, NH_2-H, Ar-H), 7.46 (t, 1H, J = 7.9 Hz, Ar-H), 7.57 (td, 1H, J = 1.4 Hz, 8.5 Hz, Ar-H), 7.62–7.67 (m, 3H, Ar-H), 7.78 (s, 1H, CH, C_4''-H); ^{13}C NMR (400 MHz, DMSO-d_6, δ, ppm): 14.63, 33.81, 59.34, 65.17, 75.90, 105.29, 112.82, 113.44, 116.67, 116.73, 119.14, 120.53, 122.36, 124.18, 124.56, 125.03, 128.46, 128.91, 131.61, 132.32, 132.72, 132.79,

https://doi.org/10.1021/acsomega.2c03528
ACS Omega 2022, 7, 28605–28617

141.49, 152.37, 153.52, 153.95, 156.81, 159.37, 159.93, 160.44, 168.46; anal. calcd for $C_{31}H_{23}O_8N$ (537.14): C = 69.27, H = 4.31, N = 2.61; found (%): C = 69.24, H = 4.33, N = 2.68.

*2-Amino-9-methyl-5-oxo-4-[2-(2-oxo-2H-chromen-3-yl-methoxy)-phenyl]-4H,5H-pyrano[3,2-c]chromene-3-carbonitrile (**12d**).* White solid; m.p. 298−300 °C; yield: 96%; solubility: DMSO; IR, KBr (cm^{-1}): 1699 (>C═O), 2194 (−CN), 3320, 3394 (NH_2-str.); ^{1}H NMR (400 MHz, DMSO-d_6, δ, ppm): 2.17 (s, 3H, CH_3- H), 4.67 (s, 1H, CH, C_4-H), 4.80 (d, 1H, J = 12.8 Hz, OCH_2-H_a), 4.93 (d, 1H, J = 12.8 Hz, OCH_2-H_b), 6.94 (t, 1H, J = 7.4 Hz, Ar-H), 7.09 (d, 1H, J = 8.2 Hz, Ar-H), 7.18−7.27 (m, 4H, Ar-H), 7.29 (s, 2H, NH_2-H), 7.34−7.41 (m, 3H, Ar-H), 7.54 (d, 1H, J = 7.8 Hz, Ar-H), 7.63 (t, 1H, J = 7.8 Hz, Ar-H), 7.92 (s, 1H, CH, C_4''-H); ^{13}C NMR (400 MHz, DMSO-d_6, δ, ppm): 14.55, 20.96, 34.28, 57.20, 60.22, 65.49, 103.61, 112.99, 113.39, 116.59, 116.62, 119.08, 121.52, 122.01, 124.02, 124.99, 128.92, 129.11, 130.73, 132.29, 133.85, 134.15, 141.30, 150.65, 153.39, 154.13, 156.53, 158.81, 159.85, 160.27; anal. calcd for $C_{30}H_{20}O_6N_2$ (504): C = 71.42, H = 4.00, N = 5.55; found (%): C = 71.35, H = 4.03, N = 5.58.

*2-Amino-9-methyl-5-oxo-4-[2-(2-oxo-2H-chromen-3-yl-methoxy)-phenyl]-4H,5H-pyrano[3,2-c]chromene-3-carboxylic Acid Methyl Ester (**12e**).* White crystalline solid; m.p. 272−274 °C; yield: 90%; solubility: DMSO, $CHCl_3$; IR, KBr (cm^{-1}): 1684, 1719 (>C═O), 3288, 3396 (NH_2-str.); ^{1}H NMR (300 MHz, DMSO-d_6, δ, ppm): 2.13 (s, 3H, CH_3-H), 3.52 (s, 3H, COOMe-CH_3-H), 4.73 (d, 1H, J = 12.6 Hz, OCH_2-H_a), 4.76 (s, 1H, CH, C_4-H), 4.82 (d, 1H, J = 12.8 Hz, OCH_2-H_b), 6.90 (t, 1H, J = 7.2 Hz, Ar-H), 6.99 (d, 1H, J = 8.1 Hz, Ar-H), 7.16 (t, 1H, J = 7.5 Hz, Ar-H), 7.24−7.30 (m, 3H, Ar-H), 7.34−7.41 (m, 3H, Ar-H), 7.48 (d, 1H, J = 7.5 Hz, Ar-H), 7.62−7.67 (m, 3H, NH_2-H, Ar-H), 7.81 (s, 1H, CH, C_4''-H); ^{13}C NMR (300 MHz, DMSO-d_6, δ, ppm): 20.92, 34.02, 50.95, 65.50, 75.86, 105.11, 113.17, 113.29, 116.52, 116.64, 119.15, 120.78, 122.04, 124.17, 125.04, 128.43, 128.92, 131.81, 132.29, 132.59, 133.54, 134.02, 141.55, 150.60, 153.48, 153.90, 156.98, 159.36, 159.91, 160.52, 168.75; anal. calcd for $C_{31}H_{23}O_8N$ (537.14): C = 69.27, H = 4.31, N = 2.61; found (%): C = 69.24, H = 4.33, N = 2.68.

*2-Amino-9-methyl-5-oxo-4-[2-(2-oxo-2H-chromen-3-yl-methoxy)-phenyl]-4H,5H-pyrano[3,2-c]chromene-3-carboxylic Acid Ethyl Ester (**12f**).* White crystalline solid; m.p. 274−276 °C; yield: 92%; solubility: DMSO, $CHCl_3$; IR, KBr (cm^{-1}): 1684, 1717 (>C═O), 3290, 3407 (NH_2-str.); ^{1}H NMR (400 MHz, DMSO-d_6, δ, ppm): 1.10 (t, 3H, J = 7.0 Hz, COOEt-CH_3-H), 2.14 (s, 3H, CH_3-H), 3.96 (q, 2H, COOEt-CH_2-H), 4.73 (d, 1H, J = 12.6 Hz, OCH_2-H_a), 4.77 (s, 1H, CH, C_4-H), 4.82 (d, 1H, J = 12.8 Hz, OCH_2-H_b), 6.90 (td, 1H, J = 0.9 Hz, 7.4 Hz, Ar-H), 6.99 (d, 1H, J = 7.7 Hz, Ar-H), 7.16 (td, 1H, J = 1.7 Hz, 8.2 Hz, Ar-H), 7.25−7.28 (m, 2H, Ar-H), 7.30 (dd, 1H, J = 1.6 Hz, 7.6 Hz, Ar-H), 7.36−7.41 (m, 3H, Ar-H), 7.51 (dd, 1H, J = 1.4 Hz, 7.6 Hz, Ar-H), 7.63−7.67 (m, 3H, NH_2-H, Ar-H), 7.82 (s, 1H, CH, C_4''-H); ^{13}C NMR (400 MHz, DMSO-d_6, δ, ppm): 14.64, 20.93, 34.28, 59.34, 65.42, 75.88, 105.12, 113.20, 116.49, 116.67, 119.16, 120.58, 122.04, 123.25, 124.17, 125.07, 128.45, 128.92, 131.74, 132.32, 132.84, 133.58, 134.05, 141.57, 150.62, 153.43, 153.92, 156.97, 159.39, 160.00, 160.59, 168.48; anal. calcd for $C_{32}H_{25}O_8N$ (551.16): C = 69.68, H = 4.57, N = 2.54; found (%): C = 69.62, H = 4.63, N = 2.58.

*2-Amino-8-methyl-5-oxo-4-[2-(2-oxo-2H-chromen-3-yl-methoxy)-phenyl]-4H,5H-pyrano[3,2-c]chromene-3-carboxylic Acid Ethyl Ester (**12g**).* White crystalline solid; m.p. 236−238 °C; yield: 94%; solubility: DMSO, $CHCl_3$; IR, KBr (cm^{-1}): 1684, 1719 (>C═O), 3315, 3430 (NH_2-str.); ^{1}H NMR (400 MHz, DMSO-d_6, δ, ppm): 1.10 (t, 3H, J = 7.0 Hz, COOEt-CH_3-H), 2.14 (s, 3H, CH_3-H), 3.96 (q, 2H, COOEt-CH_2-H), 4.73 (d, 1H, J = 12.6 Hz, OCH_2-H_a), 4.77 (s, 1H, CH, C_4-H), 4.82 (d, 1H, J = 12.8 Hz, OCH_2-H_b), 6.90 (td, 1H, J = 0.9 Hz, 7.4 Hz, Ar-H), 6.99 (d, 1H, J = 7.7 Hz, Ar-H), 7.16 (td, 1H, J = 1.7 Hz, 8.2 Hz, Ar-H), 7.25−7.28 (m, 2H, Ar-H), 7.30 (dd, 1H, J = 1.6 Hz, 7.6 Hz, Ar-H), 7.36−7.41 (m, 3H, Ar-H), 7.51 (dd, 1H, J = 1.4 Hz, 7.6 Hz, Ar-H), 7.63−7.67 (m, 3H, NH_2-H, Ar-H), 7.82 (s, 1H, CH, C_4''-H); ^{13}C NMR (400 MHz, DMSO-d_6, δ, ppm): 14.88, 21.21, 33.98, 49.06, 57.12, 65.32, 102.68, 110.69, 113.03, 116.60, 116.79, 119.07, 120.11, 121.42, 121.95, 123.98, 124.94, 125.77, 128.90, 129.07, 130.61, 131.06, 132.77, 141.43, 143.85, 152.47, 153.46, 154.40, 156.44, 158.81, 159.90, 160.33; anal. calcd for $C_{32}H_{25}O_8N$ (551.16): C = 69.68, H = 4.57, N = 2.54; found (%): C = 69.62, H = 4.63, N = 2.58.

*2-Amino-8-hydroxy-5-oxo-4-[2-(2-oxo-2H-chromen-3-yl-methoxy)-phenyl]-4H,5H-pyrano[3,2-c]chromene-3-carbonitrile (**12h**).* White amorphous solid; m.p. 302−304 °C; yield: 94%; solubility: DMSO; IR, KBr (cm^{-1}): 1667, 1700 (>C═O), 2208 (−CN), 3170, 3320 (NH_2-str.), 3461 (−OH); ^{1}H NMR (300 MHz, DMSO-d_6, δ, ppm): 4.69 (s, 1H, CH, C_4-H), 4.84 (d, 1H, J = 13.2 Hz, CH_2-H_a), 4.95 (d, 1H, J = 13.2 Hz, CH_2-H_b), 6.57 (dd, 1H, J = 2.1 Hz, 8.7 Hz, Ar-H), 6.71 (d, 1H, J = 2.4 Hz, Ar-H), 6.93 (t, 1H, J = 7.2 Hz, Ar-H), 7.06 (d, 1H, J = 8.1 Hz, Ar-H), 7.16−7.25 (m, 4H, NH_2-H, Ar-H), 7.31−7.38 (m, 3H, Ar-H), 7.55−7.65 (m, 2H, Ar-H), 7.94 (s, 1H, CH, C_4''-H), 10.65 (s, 1H, OH); ^{13}C NMR (300 MHz, DMSO-d_6, δ, ppm): 33.39, 57.37, 65.25, 99.95, 102.60, 105.08, 113.11, 113.55, 116.57, 119.12, 120.14, 121.52, 123.68, 124.13, 124.99, 128.88, 128.95, 130.40, 131.56, 132.24, 141.03, 153.39, 154.35, 154.88, 156.25, 158.83, 159.89, 160.63, 162.13; anal. calcd for $C_{29}H_{18}O_7N_2$ (506.11): C = 68.77, H = 3.58, N = 5.53; found (%): C = 68.71, H = 3.61, N = 5.56.

*2-Amino-8-hydroxy-5-oxo-4-[2-(2-oxo-2H-chromen-3-yl-methoxy)-phenyl]-4H,5H-pyrano[3,2-c]chromene-3-carboxylic Acid Methyl Ester (**12i**).* White crystalline solid; m.p. 242−244 °C; yield: 70%; solubility: DMSO, $CHCl_3$; IR, KBr (cm^{-1}): 1686 (>C═O), 3298, 3421 (NH_2-str.), 3492 (−OH); ^{1}H NMR (300 MHz, DMSO-d_6, δ, ppm): 3.51 (s, 3H, COOEt-CH_3-H), 4.75 (s, 1H, CH, C_4-H), 4.76 (d, 1H, J = 12.9 Hz, CH_2-H_a), 4.86 (d, 1H, J = 13.2 Hz, CH_2-H_b), 6.51 (dd, 1H, J = 2.1 Hz, 8.7 Hz, Ar-H), 6.68 (d, 1H, J = 2.1 Hz, Ar-H), 6.88 (t, 1H, J = 7.2 Hz, Ar-H), 6.96 (d, 1H, J = 8.1 Hz, Ar-H), 7.14 (t, 1H, J = 7.8 Hz, Ar-H), 7.25−7.28 (m, 2H, Ar-H), 7.34−7.41 (m, 2H, Ar-H), 7.50 (d, 1H, J = 6.6 Hz, Ar-H), 7.62−7.67 (m, 3H, NH_2-H, Ar-H), 7.77 (s, 1H, CH, C_4''-H), 10.58 (s, 1H, OH); ^{13}C NMR (300 MHz, DMSO-d_6, δ, ppm): 33.47, 50.94, 65.21, 76.08, 101.58, 102.53, 105.30, 112.93, 113.35, 116.61, 119.15, 120.71, 123.67, 124.28, 125.01, 128.29, 128.87, 132.13, 132.29, 132.67, 141.31, 153.49, 154.28, 154.61, 156.73, 159.42, 159.94, 160.88, 161.85, 168.80; anal. calcd for $C_{30}H_{21}O_9N$ (539.12): C = 66.79, H = 3.92, N = 2.60; found (%): C = 66.74, H = 3.94, N = 2.56.

*2-Amino-8-hydroxy-5-oxo-4-[2-(2-oxo-2H-chromen-3-yl-methoxy)-phenyl]-4H,5H-pyrano[3,2-c]chromene-3-carboxylic Acid Ethyl Ester (**12j**).* White crystalline solid; m.p. 248−250 °C; yield: 74%; solubility: DMSO, $CHCl_3$; IR, KBr (cm^{-1}): 1685 (>C═O), 3283, 3294 (NH_2-str.), 3648 (−OH); ^{1}H NMR (300 MHz, DMSO-d_6, δ, ppm): 1.08 (t, 3H, J = 7.2 Hz, COOEt-CH_3-H), 3.95 (q, 2H, COOEt-CH_2-H), 4.75 (s,

https://doi.org/10.1021/acsomega.2c03528
ACS Omega 2022, 7, 28605−28617

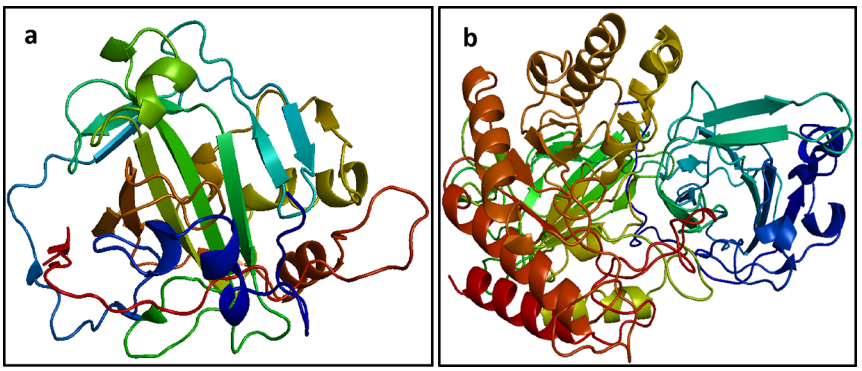

Figure 4. (a) Carbonic anhydrase (PDB ID: 1BN1) and (b) β-glucuronidase (PDB ID: 5CZK).

1H, CH, C_4-H), 4.76 (d, 1H, J = 12.9 Hz, CH_2-H_a), 4.86 (d, 1H, J = 13.2 Hz, CH_2-H_b), 6.51 (dd, 1H, J = 2.1 Hz, 8.7 Hz, Ar-H), 6.68 (d, 1H, J = 2.1 Hz, Ar-H), 6.88 (t, 1H, J = 7.2 Hz, Ar-H), 6.96 (d, 1H, J = 8.1 Hz, Ar-H), 7.14 (td, 1H, J = 1.5 Hz, 8.7 Hz, Ar-H), 7.25−7.28 (m, 2H, Ar-H), 7.34−7.41 (m, 2H, Ar-H), 7.50 (d, 1H, J = 6.6 Hz, Ar-H), 7.62−7.67 (m, 3H, NH_2-H, Ar-H), 7.79 (s, 1H, CH, C_4''-H), 10.58 (s, 1H, OH); ^{13}C NMR (300 MHz, DMSO-d_6, δ, ppm): 14.63, 33.48, 59.29, 65.10, 76.09, 101.56, 102.52, 105.30, 112.80, 113.36, 116.62, 119.15, 120.50, 123.64, 124.25, 125.02, 128.29, 128.85, 132.06, 132.29, 132.67, 141.32, 153.48, 154.28, 154.59, 156.70, 159.42, 159.94, 160.93, 161.86, 168.53; anal. calcd for $C_{31}H_{23}O_9N$ (553.14): C = 67.27, H = 4.19, N = 2.53; found (%): C = 67.23, H = 4.24, N = 2.56.

*2-Amino-4-[5-bromo-2-(6-bromo-2-oxo-2H-chromen-3-ylmethoxy)-phenyl]-5-oxo-4H,5H-pyrano[3,2-c]chromene-3-carbonitrile (**12k**).* White solid; m.p. 290−292 °C; yield: 52%; solubility: DMSO, $CHCl_3$; IR, KBr (cm^{-1}): 1717 (>C═O), 2192 (−CN), 3178, 3336 (NH_2-str.); ^{1}H NMR (300 MHz, DMSO-d_6, δ, ppm): 4.70 (s, 1H, C_4-H), 4.79 (d, 1H, J = 12.6 Hz, CH_2-H_a), 4.92 (d, 1H, J = 12.6 Hz, CH_2-H_b), 7.08 (d, 1H, J = 9.3 Hz, Ar-H), 7.12 (d, 1H, J = 7.8 Hz, Ar-H), 7.29−7.33 (m, 3H, Ar-H), 7.40−7.43 (m, 4H, NH_2-H, Ar-H), 7.60 (t, 1H, J = 8.4 Hz, Ar-H), 7.70 (d, 1H, J = 2.4 Hz, Ar-H), 7.77 (dd, 1H, J = 2.4 Hz, 8.7 Hz, Ar-H), 7.87 (s, 1H, CH, C_4''-H); ^{13}C NMR (300 MHz, DMSO-d_6, δ, ppm): 33.95, 56.32, 65.64, 102.94, 112.99, 113.18, 115.45, 116.61, 116.86, 118.94, 119.92, 120.86, 122.34, 124.60, 124.83, 130.99, 131.65, 132.95, 133.02, 133.38, 134.69, 140.43, 152.46, 152.51, 154.34, 155.86, 158.89, 159.32, 160.13; anal. calcd for $C_{29}H_{16}O_6N_2Br_2$ (648.26): C = 53.73, H = 2.49, N = 4.32; found (%): C = 53.68, H = 2.54, N = 4.28.

*2-Amino-4-[5-bromo-2-(6-bromo-2-oxo-2H-chromen-3-ylmethoxy)-phenyl]-9-methyl-5-oxo-4H,5H-pyrano[3,2-c]-chromene-3-carbonitrile (**12l**).* White solid; m.p. >340 °C; yield: 54%; solubility: DMSO, $CHCl_3$; IR, KBr (cm^{-1}): 1718 (>C═O), 2197 (−CN), 3310, 3387 (NH_2-str.); ^{1}H NMR (300 MHz, DMSO-d_6, δ, ppm): 2.39 (s, 3H, CH_3-H), 4.63 (s, 1H, CH, C_4-H), 4.76 (d, 1H, J = 12.6 Hz, OCH_2-H_a), 4.90 (d, 1H, J = 12.3 Hz, OCH_2-H_b), 6.86 (d, 1H, J = 8.1 Hz, Ar-H), 7.08 (d, 1H, J = 9.3 Hz, Ar-H), 7.21−7.33 (m, 5H, NH_2-H, Ar-H), 7.41−7.44 (m, 2H, Ar-H), 7.67 (d, 1H, J = 2.4 Hz, Ar-H), 7.77−7.81 (m, 2H, Ar-H & CH, C_4''-H); ^{13}C NMR (300 MHz, DMSO-d_6, δ, ppm): 14.55, 20.96, 34.28, 57.20, 60.22, 65.49, 103.61, 112.99, 113.39, 116.59, 116.62, 119.08, 121.52, 122.01, 124.02, 124.99, 128.92, 129.11, 130.73, 132.29, 133.85, 134.15, 141.30, 150.65, 153.39, 154.13, 156.53, 158.81, 159.85, 160.27; anal. calcd for $C_{30}H_{18}O_6N_2Br_2$ (662.86): C = 54.41, H = 2.74, N = 4.23; found (%): C = 54.38, H = 2.79, N = 4.28.

*2-Amino-4-[5-bromo-2-(6-bromo-2-oxo-2H-chromen-3-ylmethoxy)-phenyl]-8-methyl-5-oxo-4H,5H-pyrano[3,2-c]-chromene-3-carbonitrile (**12m**).* White solid; m.p. 300−302 °C; yield: 48%; solubility: DMSO, $CHCl_3$; IR, KBr (cm^{-1}): 1713 (>C═O), 2194 (−CN), 3312, 3390 (NH_2-str.); ^{1}H NMR (300 MHz, DMSO-d_6, δ, ppm): 2.39 (s, 3H, CH_3-H), 4.63 (s, 1H, CH, C_4-H), 4.76 (d, 1H, J = 12.6 Hz, OCH_2-H_a), 4.90 (d, 1H, J = 12.3 Hz, OCH_2-H_b), 6.86 (d, 1H, J = 8.1 Hz, Ar-H), 7.08 (d, 1H, J = 9.3 Hz, Ar-H), 7.21−7.33 (m, 5H, NH_2-H, Ar-H), 7.41−7.44 (m, 2H, Ar-H), 7.67 (d, 1H, J = 2.4 Hz, Ar-H), 7.77−7.81 (m, 2H, Ar-H & CH, C_4''-H); ^{13}C NMR (300 MHz, DMSO-d_6, δ, ppm): 21.79, 34.23, 56.26, 65.69, 101.90, 110.60, 112.86, 115.40, 116.56, 116.81, 118.91, 119.96, 120.84, 121.97, 124.77, 125.65, 130.97, 131.60, 132.98, 133.30, 134.70, 140.62, 143.97, 152.50, 152.59, 154.49, 155.99, 158.91, 159.31, 160.29; anal. calcd for $C_{30}H_{18}O_6N_2Br_2$ (662.86): C = 54.41, H = 2.74, N = 4.23; found (%): C = 54.38, H = 2.79, N = 4.28.

Biological Evaluation. *Carbonic Anhydrase Inhibition Assay.* This assay shows the hydrolytic conversion of 4-NPA (4-nitrophenyl acetate) to 4-nitrophenol and CO_2. The above conversion was done (at 25 °C) in buffer carrying HEPES and Tris−HCl with a concentration of 20 mM at pH 7.4 for all samples. The reaction mixture was held with HEPES-Tris solution (140 μL), carbonic anhydrase (20 μL), and a sample solution of compound in DMSO (20 μL) and 4-NPA (20 μL) in ethanol at a concentration of 0.7 mM.

The reaction was initialized by adding 4-NPA to the previously incubated test sample for 15 min to 6 h and carried out utilizing 96-well plates. The data reported in Table 2a shows the inhibition after 15 min of incubation as there is no difference of inhibitory power when the enzyme and inhibitor are kept for a long period in incubation. The amount of product obtained during the reaction was recorded for 30 min in a spectrophotometer with an interval of 1 min at 400 nm.[73]

β-Glucuronidase Inhibition Assay. The assay for inhibition of β-glucuronidase was performed utilizing a conventionally reported methodology with slight amendments.[74] In short, 100 μL of β-glucuronidase (0.1 M of 986.4 units/mL with phosphate-buffered solution at pH 7) and 340 μL of test sample solution/reference standard of varying concentrations with the same buffer were pre-incubated for 15 min at 37 °C. Sixty microliters of p-nitrophenyl-(β)-D-glucuronide (3.15 mg/mL buffered at pH 7 in 0.1 M phosphate buffer) was put onto the aforementioned solution and further incubated for 50 min under the same parameters. The developed color was

https://doi.org/10.1021/acsomega.2c03528
ACS Omega 2022, 7, 28605−28617

perceived at 405 nm in absorbance spectrum. Control assay was performed without test samples, and finally, % age inhibition was premediated.

Molecular Docking Studies (Methodology). Molecular docking studies were performed via ICM v3.8-7d (Molsoft L.L.C., La Jolla, CA)[75] to evaluate the binding tendency of test compounds into the active pocket of carbonic anhydrase and β-glucuronidase. The 3D structures of carbonic anhydrase and β-glucuronidase were retrieved from Protein Data Bank with accession codes 1BN1 (resolution: 1.66 Å)[76] and 5CZK (resolution: 2.39 Å)[77] (Figure 4). The receptor preparation tool of ICM v3.8-7d (Molsoft L.L.C., La Jolla, CA) was used to prepare protein for docking that involved (i) optimization of hydrogen atoms, (ii) addition of Gasteiger charges, and (iii) removal of water molecules and reference ligand. The energy optimization was carried out using the default force field. The three-dimensional (3D) structures of compounds were modeled using the ligedit tool of ICM and later optimized.[75]

The active pocket of protein was specified through a grid box, and compounds were docked into the pocket to evaluate their binding interaction with pocket residues. The 10 best docked conformations were generated for each compound.

The view of the docking results and the analysis of their surface with graphical representations were done using ICM, while the ligand interaction module of Discovery Studio Visualizer was used to calculate the 2D ligand−enzyme interactions.

■ ASSOCIATED CONTENT

Supporting Information

The Supporting Information is available free of charge at https://pubs.acs.org/doi/10.1021/acsomega.2c03528.

General mechanism of carbonic anhydrase inhibition by coumarin analogs; optimization of reaction parameters for the preparation of model compound **12a**; binding interaction of potent inhibitors with active site residues of hCA II and β-glucoronidase; 2D view for the binding interaction pattern of compounds **12d**, **12e**, **12g**, and **12i** with active site residues of β-glucoronidase; ^{1}H NMR and ^{13}C NMR spectra of **9a**, **9b**, and **12a−12m** (PDF)

■ AUTHOR INFORMATION

Corresponding Authors

Zahid Shafiq − *Institute of Chemical Sciences, Organic Chemistry Division, Bahauddin Zakariya University, Multan 60800, Pakistan; Department of Pharmaceutical & Medicinal Chemistry, University of Bonn, D-53121 Bonn, Germany;* orcid.org/0000-0003-4088-8297; Email: zahidshafiq@bzu.edu.pk

Muhammad Yaqub − *Institute of Chemical Sciences, Organic Chemistry Division, Bahauddin Zakariya University, Multan 60800, Pakistan*; Phone: +92-3084758848; Email: mayaqub2@yahoo.com

Authors

Nadia Arif − *Institute of Chemical Sciences, Organic Chemistry Division, Bahauddin Zakariya University, Multan 60800, Pakistan*

Khalid Mahmood − *Institute of Chemical Sciences, Organic Chemistry Division, Bahauddin Zakariya University, Multan 60800, Pakistan*

Muhammad Rafiq − *Institute of Chemical Sciences, Organic Chemistry Division, Bahauddin Zakariya University, Multan 60800, Pakistan*

Sadia Naz − *Department of Chemistry, COMSATS University Islamabad, Abbottabad Campus, Abbottabad 22060, Pakistan*

Sohail Anjum Shahzad − *Department of Chemistry, COMSATS University Islamabad, Abbottabad Campus, Abbottabad 22060, Pakistan;* orcid.org/0000-0002-4226-3023

Umar Farooq − *Department of Chemistry, COMSATS University Islamabad, Abbottabad Campus, Abbottabad 22060, Pakistan*

Ali H. Bahkali − *Department of Botany and Microbiology, College of Science, King Saud University, Riyadh 11451, Saudi Arabia*

Abdallah M. Elgorban − *Department of Botany and Microbiology, College of Science, King Saud University, Riyadh 11451, Saudi Arabia*

Ahmed El-Gokha − *Department of Pharmaceutical & Medicinal Chemistry, University of Bonn, D-53121 Bonn, Germany; Chemistry Department, Faculty of Science, Menoufia University, Shebin El-Kom 32512, Egypt*

Complete contact information is available at: https://pubs.acs.org/10.1021/acsomega.2c03528

Author Contributions

The manuscript was written through the contributions of all authors. All authors have given approval to the final version of the manuscript.

Notes

The authors declare no competing financial interest.

■ ACKNOWLEDGMENTS

The authors extend their appreciation to the Researchers Supporting Project (number RSP-2021/15), King Saud University, Riyadh, Saudi Arabia. Z.S. is thankful to the Alexander von Humboldt Foundation for the award of Georg Forster Research Fellowship for Experienced Researchers.

■ REFERENCES

(1) Bai, Y.; Chen, L.; Cao, Y.-F.; Hou, X.-D.; Jia, S.-N.; Zhou, Q.; He, Y.-Q.; Hou, J. Beta-glucuronidase inhibition by constituents of mulberry bark. *Planta Med.* **2021**, *87*, 631−641.

(2) Tomatsu, S.; Montaño, A. M.; Dung, V. C.; Grubb, J. H.; Sly, W. S. Mutations and polymorphisms in GUSB gene in mucopolysaccharidosis VII (Sly Syndrome). *Hum. Mutat.* **2009**, *30*, 511−519.

(3) Hradec, E.; Petřík, R.; Pezlarová, J. The activity of β-glucuronidase in cases of bladder neoplasms. *J. Urol.* **1965**, *94*, 430−435.

(4) Wang, J.; Zhang, L.; Su, Y.; Qu, Y.; Cao, Y.; Qin, W.; Liu, Y. A Novel Fluorescent Probe Strategy Activated by β-Glucuronidase for Assisting Surgical Resection of Liver Cancer. *Anal. Chem.* **2022**, 7012.

(5) Ozawa-Umeta, H.; Kishimoto, A.; Imaizumi, A.; Hashimoto, T.; Asakura, T.; Kakeya, H.; Kanai, M. Curcumin β-D-glucuronide exhibits anti−tumor effects on oxaliplatin-resistant colon cancer with less toxicity in vivo. *Cancer Sci.* **2020**, *111*, 1785−1793.

(6) Wei, X.; Li, J.; Yang, X.; Dong, B.; Geng, B.; Li, Z.; Hu, X.; Ding, B.; Zhang, J.; Yan, M. An enzyme-activated two-photon ratiometric fluorescent probe with lysosome targetability for imaging β-glucuronidase in colon cancer cells and tissue. *Anal. Chim. Acta* **2022**, *1192*, No. 339354.

(7) Li, T.; Li, G.; Su, Z.; Liu, J.; Wang, P. Recent advances of sensing strategies for the detection of β-glucuronidase activity. *Anal. Bioanal. Chem.* **2022**, 1−17.
(8) Juan, T.-Y.; Roffler, S. R.; Hou, H.-S.; Huang, S.-M.; Chen, K.-C.; Leu, Y.-L.; Prijovich, Z. M.; Yu, C.-P.; Wu, C.-C.; Sun, G.-H.; Cha, T. L. Antiangiogenesis targeting tumor microenvironment synergizes glucuronide prodrug antitumor activity. *Clin. Cancer Res.* **2009**, *15*, 4600−4611.
(9) Piwowarski, J. P.; Stanisławska, I.; Granica, S.; Stefańska, J.; Kiss, A. K. Phase II conjugates of urolithins isolated from human urine and potential role of β-glucuronidases in their disposition. *Drug Metab. Dispos.* **2017**, *45*, 657−665.
(10) Feng, L.; Yang, Y.; Huo, X.; Tian, X.; Feng, Y.; Yuan, H.; Zhao, L.; Wang, C.; Chu, P.; Long, F.; Wang, W.; Ma, X. Highly selective NIR probe for intestinal β-glucuronidase and high-throughput screening inhibitors to therapy intestinal damage. *ACS Sens.* **2018**, *3*, 1727−1734.
(11) Kraan, C.; Cornish, K.; Bui, Q.; Li, X.; Slater, H.; Godler, D. β-glucuronidase mRNA levels are correlated with gait and working memory in premutation females: Understanding the role of FMR1 premutation alleles. *Sci. Rep.* **2016**, *6*, 1−9.
(12) Zhang, L. T.; Westblade, L. F.; Iqbal, F.; Taylor, M. R.; Chung, A.; Satlin, M. J.; Magruder, M.; Edusei, E.; Albakry, S.; Botticelli, B.; Robertson, A.; Alston, T.; Dadhania, D. M.; Lubetzky, M.; Hirota, S. A.; Greenway, S. C.; Lee, J. R. Gut microbiota profiles and fecal beta-glucuronidase activity in kidney transplant recipients with and without post-transplant diarrhea. *Clin. Transplant.* **2021**, *35*, No. e14260.
(13) Kunihiro, A. G.; Luis, P. B.; Brickey, J. A.; Frye, J. B.; Chow, H.-H. S.; Schneider, C.; Funk, J. L. Beta-glucuronidase catalyzes deconjugation and activation of curcumin-glucuronide in bone. *J. Nat. Prod.* **2019**, *82*, 500−509.
(14) Panagiotopoulou, E. C.; Fouzas, S.; Douros, K.; Triantaphyllidou, I. E.; Malavaki, C.; Priftis, K. N.; Karamanos, N. K.; Anthracopoulos, M. B. Increased β-glucuronidase activity in bronchoalveolar lavage fluid of children with bacterial lung infection: A case−control study. *Respirology* **2015**, *20*, 1248−1254.
(15) Sui, Y.; Wu, J.; Chen, J. The Role of Gut Microbial β-Glucuronidase in Estrogen Reactivation and Breast Cancer. *Front. Cell Dev. Biol.* **2021**, *9*, No. 631552.
(16) Cheng, K.-W.; Tseng, C.-H.; Chen, I.-J.; Huang, B.-C.; Liu, H.-J.; Ho, K.-W.; Lin, W.-W.; Chuang, C.-H.; Huang, M.-Y.; Leu, Y.-L.; Roffler, S. R.; Wang, J. Y.; Chen, Y. L.; Cheng, T. L. Inhibition of gut microbial β-glucuronidase effectively prevents carcinogen-induced microbial dysbiosis and intestinal tumorigenesis. *Pharmacol. Res.* **2022**, *177*, No. 106115.
(17) Haefling, B. R. *The role of beta-glucuronidase in enterohepatic recycling and prostate cancer progression*. University of British Columbia 2021, DOI: 10.14288/1.0402630.
(18) Güller, U.; Beydemir, Ş.; Küfrevioğlu, Ö. İ. In vitro and in silico interactions of antiulcer, glucocorticoids and urological drugs on human carbonic anhydrase I and II isozymes. *Biopharm. Drug Dispos.* **2022**, *43*, 47−56.
(19) Nocentini, A.; Supuran, C. T.; Capasso, C. An overview on the recently discovered iota-carbonic anhydrases. *J. Enzyme Inhib. Med. Chem.* **2021**, *36*, 1988−1995.
(20) Supuran, C. T. Carbonic anhydrases and metabolism. *Metabolites* **2018**, *8*, 25.
(21) Supuran, C.; Scozzafava, A. *Expert Opin. Ther. Pat.* **2002**, *12*, 217.
(22) Pastorekova, S.; Parkkila, S.; Pastorek, J.; Supuran, C. T. Carbonic anhydrases: current state of the art, therapeutic applications and future prospects. *J. Enzyme Inhib. Med. Chem.* **2004**, *19*, 199−229.
(23) Supuran, C. T. Carbonic anhydrase inhibitors in the treatment and prophylaxis of obesity. *Expert Opin. Ther. Pat.* **2003**, *13*, 1545−1550.
(24) Angeli, A.; di Cesare Mannelli, L.; Lucarini, E.; Peat, T. S.; Ghelardini, C.; Supuran, C. T. Design, synthesis and X-ray crystallography of selenides bearing benzenesulfonamide moiety with neuropathic pain modulating effects. *Eur. J. Med. Chem.* **2018**, *154*, 210−219.
(25) Di Cesare Mannelli, L.; Micheli, L.; Carta, F.; Cozzi, A.; Ghelardini, C.; Supuran, C. T. Carbonic anhydrase inhibition for the management of cerebral ischemia: in vivo evaluation of sulfonamide and coumarin inhibitors. *J. Enzyme Inhib. Med. Chem.* **2016**, *31*, 894−899.
(26) Fuentes-Aguilar, A.; Merino-Montiel, P.; Montiel-Smith, S.; Meza-Reyes, S.; Vega-Báez, J. L.; Puerta, A.; Fernandes, M. X.; Padrón, J. M.; Petreni, A.; Nocentini, A.; Supuran, C. T.; López, Ó.; Fernández-Bolaños, J. G. 2-Aminobenzoxazole-appended coumarins as potent and selective inhibitors of tumour-associated carbonic anhydrases. *J. Enzyme Inhib. Med. Chem.* **2022**, *37*, 168−177.
(27) Lemon, N.; Canepa, E.; Ilies, M. A.; Fossati, S. Carbonic Anhydrases as Potential Targets Against Neurovascular Unit Dysfunction in Alzheimer's Disease and Stroke. *Front. Aging Neurosci.* **2021**, 785.
(28) Dzobo, K. The role of natural products as sources of therapeutic agents for innovative drug discovery. *Compr. Pharmacol.* **2022**, 408−422.
(29) Shi, Y.-L.; Shi, M. The synthesis of chromenes, chromanes, coumarins and related heterocycles via tandem reactions of salicylic aldehydes or salicylic imines with α, β-unsaturated compounds. *Org. Biomol. Chem.* **2007**, *5*, 1499−1504.
(30) Sahni, T.; Sharma, S.; Verma, D.; Kaur, P. Overview of Coumarins and its Derivatives: Synthesis and Biological Activity. *Lett. Org. Chem.* **2021**, *18*, 880−902.
(31) Costa, M.; Dias, T. A.; Brito, A.; Proença, F. Biological importance of structurally diversified chromenes. *Eur. J. Med. Chem.* **2016**, *123*, 487−507.
(32) Konda, S. K.; Gutam, M.; Thalari, G.; Bhoga, S.; Nayaki, S. R.; Mattela, K.; Krupadanam, G. L. D. Synthesis, characterization, and antifungal activity of novel chromene oxadiazole based dithiocarbamates. *Synth. Commun.* **2022**, *52*, 577−584.
(33) Oktavia, S. H.; Cahyana, A. H.; Hapsari, M.; Yunarti, R. T.; Liandi, A. R. Synthesis and antimicrobial activity of spiro-oxindole-chromene derivative compounds based curcuminoid and chalcone. *Rasayan J. Chem.* **2021**, *14*, 1990−1997.
(34) Ilyinaa, I. V.; Patrushevaa, O. S.; Zarubaevb, V. V.; Volchoa, K. P.; Salakhutdinova, N. F., *F-And OH-containing Isopulegol-derived Octahydro-2H-chromenes as Agents Against Influenza A Virus*. 2021.
(35) Kantharaju, K.; Khatavi, S. Y. A green method synthesis and antimicrobial activity of 2-amino-4H-chromene derivatives. *Asian J. Chem.* **2018 Jul 1**, *30*, 1496−1502.
(36) Chaudhari, B. B.; Bali, A.; Balaini, A. Design and Synthesis of Novel Anti-inflammatory/Anti-ulcer Hybrid Molecules with Anti-oxidant Activity. *Med. Chem.* **2021**, *17*, 994−1006.
(37) Dos Reis, G. O.; da Rosa, J. S.; Lubschinksi, T. L.; Martin, E. F.; Sandjo, L. P.; Dalmarco, E. M.Evidence that the anti-inflammatory effect of 4-aryl-4H-chromenes is linked to macrophage repolarization. *Fundam. Clin. Pharmacol.* 2022, DOI: 10.1111/fcp.12809
(38) Elgaafary, M.; Lehner, J.; Fouda, A. M.; Hamed, A.; Ulrich, J.; Simmet, T.; Syrovets, T.; El-Agrody, A. M. Synthesis and evaluation of antitumor activity of 9-methoxy-1H-benzo [f] chromene derivatives. *Bioorg. Chem.* **2021**, *116*, No. 105402.
(39) Narender, T.; Gupta, S. A convenient and biogenetic type synthesis of few naturally occurring chromeno dihydrochalcones and their in vitro antileishmanial activity. *Bioorg. Med. Chem. Lett.* **2004**, *14*, 3913−3916.
(40) Luque-Agudo, V.; Albarrán-Velo, J.; Light, M. E.; Padrón, J. M.; Román, E.; Serrano, J. A.; Gil, M. V. Synthesis and antiproliferative activity of new 2-glyco-3-nitro-2H-chromenes. *Bioorg. Chem.* **2019**, *87*, 112−116.
(41) Al-Masoudi, N. A.; Mohammed, H. H.; Hamdy, A. M.; Akrawi, O. A.; Eleya, N.; Spannenberg, A.; Pannecouque, C.; Langer, P. Synthesis and anti-HIV Activity of New Fused Chromene Derivatives Derived from 2-Amino-4-(1-naphthyl)-5-oxo-4H, 5H-pyrano [3, 2-c] chromene-3-carbonitrile. *Z. Naturforsch.* **2013**, *B, 68*, 229−238.

https://doi.org/10.1021/acsomega.2c03528
ACS Omega 2022, 7, 28605−28617

(42) Anaikutti, P.; Selvaraj, M.; Prabhakaran, J.; Pooventhiran, T.; Jeyakumar, T. C.; Thomas, R.; Makam, P. Indolyl-4H-chromenes: Multicomponent one-pot green synthesis, in vitro and in silico, anticancer and antioxidant studies. *J. Mol. Struct.* **2022**, No. 133464.
(43) Katiyar, M. K.; Dhakad, G. K.; Arora, S.; Bhagat, S.; Katyal, T.; Kumar, R. Synthetic Strategies and Pharmacological Activities of Chromene and Its Derivatives: An Overview. *J. Mol. Struct.* **2022**, No. 133012.
(44) Ibrahim, H. S.; Abdelrahman, M. A.; Nocentini, A.; Bua, S.; Abdel-Aziz, H. A.; Supuran, C. T.; Abou-Seri, S. M.; Eldehna, W. M. Insights into the effect of elaborating coumarin-based aryl enaminones with sulfonamide or carboxylic acid functionality on carbonic anhydrase inhibitory potency and selectivity. *Bioorg. Chem.* **2022**, No. 105888.
(45) Milite, C.; Amendola, G.; Nocentini, A.; Bua, S.; Cipriano, A.; Barresi, E.; Feoli, A.; Novellino, E.; Da Settimo, F.; Supuran, C. T.; Castellano, S. Novel 2-substituted-benzimidazole-6-sulfonamides as carbonic anhydrase inhibitors: synthesis, biological evaluation against isoforms I, II, IX and XII and molecular docking studies. *J. Enzyme Inhib. Med. Chem.* **2019**, *34*, 1697−1710.
(46) Supuran, C. T. Drug interaction considerations in the therapeutic use of carbonic anhydrase inhibitors. *Expert Opin. Drug Metab. Toxicol.* **2016**, *12*, 423−431.
(47) Supuran, C. T. Carbonic anhydrase inhibitors and their potential in a range of therapeutic areas. *Expert Opin. Ther. Pat.* **2018**, *28*, 709−712.
(48) Ali, M.; Bozdag, M.; Farooq, U.; Angeli, A.; Carta, F.; Berto, P.; Zanotti, G.; Supuran, C. T. Benzylaminoethyureido-tailed benzenesulfonamides: Design, synthesis, kinetic and X-ray investigations on human carbonic anhydrases. *Int. J. Mol. Sci.* **2020**, *21*, 2560.
(49) Maresca, A.; Temperini, C.; Vu, H.; Pham, N. B.; Poulsen, S.-A.; Scozzafava, A.; Quinn, R. J.; Supuran, C. T. Non-zinc mediated inhibition of carbonic anhydrases: coumarins are a new class of suicide inhibitors. *J. Am. Chem. Soc.* **2009**, *131*, 3057−3062.
(50) Maresca, A.; Temperini, C.; Pochet, L.; Masereel, B.; Scozzafava, A.; Supuran, C. T. Deciphering the mechanism of carbonic anhydrase inhibition with coumarins and thiocoumarins. *J. Med. Chem.* **2010**, *53*, 335−344.
(51) Maresca, A.; Supuran, C. T. Coumarins incorporating hydroxy- and chloro-moieties selectively inhibit the transmembrane, tumor-associated carbonic anhydrase isoforms IX and XII over the cytosolic ones I and II. *Bioorg. Med. Chem. Lett.* **2010**, *20*, 4511−4514.
(52) Supuran, C. T. Carbonic anhydrases: novel therapeutic applications for inhibitors and activators. *Nat. Rev. Drug Discov.* **2008**, *7*, 168−181.
(53) Supuran, C. T. Structure and function of carbonic anhydrases. *Biochem. J.* **2016**, *473*, 2023−2032.
(54) Fois, B.; Distinto, S.; Meleddu, R.; Deplano, S.; Maccioni, E.; Floris, C.; Rosa, A.; Nieddu, M.; Caboni, P.; Sissi, C.; Angeli, A.; Supuran, C. T.; Cottiglia, F. Coumarins from Magydaris pastinacea as inhibitors of the tumour-associated carbonic anhydrases IX and XII: isolation, biological studies and in silico evaluation. *J. Enzyme Inhib. Med. Chem.* **2020**, *35*, 539−548.
(55) Melis, C.; Distinto, S.; Bianco, G.; Meleddu, R.; Cottiglia, F.; Fois, B.; Taverna, D.; Angius, R.; Alcaro, S.; Ortuso, F.; Gaspari, M.; Angeli, A.; del Prete, S.; Capasso, C.; Supuran, C. T.; Maccioni, E. Targeting tumor associated carbonic anhydrases IX and XII: highly isozyme selective coumarin and psoralen inhibitors. *ACS Med. Chem. Lett.* **2018**, *9*, 725−729.
(56) Meleddu, R.; Deplano, S.; Maccioni, E.; Ortuso, F.; Cottiglia, F.; Secci, D.; Onali, A.; Sanna, E.; Angeli, A.; Angius, R.; Alcaro, S.; Supuran, C. T.; Distinto, S. Selective inhibition of carbonic anhydrase IX and XII by coumarin and psoralen derivatives. *J. Enzyme Inhib. Med. Chem.* **2021**, *36*, 685−692.
(57) Kartsev, V.; Geronikaki, A.; Bua, S.; Nocentini, A.; Petrou, A.; Lichitsky, B.; Frasinyuk, M.; Leitans, J.; Kazaks, A.; Tars, K.; Supuran. Extending the inhibition profiles of coumarin-based compounds against human carbonic anhydrases: Synthesis, biological, and in silico evaluation. *Molecules* **2019**, *24*, 3580.
(58) Khan, I.; Khan, A.; Halim, S. A.; Khan, M.; Zaib, S.; Al-Yahyaei, B. E. M.; Al-Harrasi, A.; Ibrar, A. Utilization of the common functional groups in bioactive molecules: Exploring dual inhibitory potential and computational analysis of keto esters against α-glucosidase and carbonic anhydrase-II enzymes. *Int. J. Biol. Macromol.* **2021**, *167*, 233−244.
(59) Rafiq, K.; Ur Rehman, N.; Halim, S. A.; Khan, M.; Khan, A.; Al-Harrasi, A. Design, Synthesis and Molecular Docking Study of Novel 3-Phenyl-β-Alanine-Based Oxadiazole Analogues as Potent Carbonic Anhydrase II Inhibitors. *Molecules* **2022**, *27*, 816.
(60) Hou, Z.; Li, C.; Liu, Y.; Zhang, M.; Wang, Y.; Fan, Z.; Guo, C.; Lin, B.; Liu, Y. Design, synthesis and biological evaluation of carbohydrate-based sulphonamide derivatives as topical antiglaucoma agents through selective inhibition of carbonic anhydrase II. *J. Enzyme Inhib. Med. Chem.* **2020**, *35*, 383−390.
(61) Abid, O.; Imran, S.; Taha, M.; Ismail, N. H.; Jamil, W.; Kashif, S. M.; Khan, K. M.; Yusoff, J. Synthesis, β-glucuronidase inhibition and molecular docking studies of cyano-substituted bisindole hydrazone hybrids. *Mol. Diversity* **2021**, *25*, 995−1009.
(62) Taha, M.; Khan, A. A.; Rahim, F.; Imran, S.; Salahuddin, M.; Uddin, N.; Khan, K. M.; Shah, S. A. A.; Zafar, A.; Zakaria, Z. A. Synthesis of new 1, 2-disubstituted benzimidazole analogs as potent inhibitors of β-Glucuronidase and in silico study. *Arab. J. Chem.* **2022**, *15*, No. 103505.
(63) Yousuf, M.; Shaikh, N. N.; Ul-Haq, Z.; Choudhary, M. I. Bioinformatics: A rational combine approach used for the identification and in-vitro activity evaluation of potent β-Glucuronidase inhibitors. *PLoS One* **2018**, *13*, No. e0200502.
(64) Singh, R.; Bhardwaj, V. K.; Purohit, R. Computational targeting of allosteric site of MEK1 by quinoline-based molecules. *Cell Biochem. Funct.* **2022**, 481.
(65) Singh, R.; Bhardwaj, V. K.; Das, P.; Purohit, R. Identification of 11β-HSD1 inhibitors through enhanced sampling methods. *Chem. Commun.* **2022**, *58*, 5005−5008.
(66) Bhardwaj, V. K.; Oakley, A.; Purohit, R. Mechanistic behavior and subtle key events during DNA clamp opening and closing in T4 bacteriophage. *Int. J. Biol. Macromol.* **2022**, *208*, 11−19.
(67) Kumar, S.; Bhardwaj, V. K.; Singh, R.; Das, P.; Purohit, R. Identification of acridinedione scaffolds as potential inhibitor of DENV-2 C protein: An in silico strategy to combat dengue. *J. Cell. Biochem.* **2022**, 935.
(68) Bhardwaj, V. K.; Purohit, R. A lesson for the maestro of the replication fork: Targeting the protein-binding interface of proliferating cell nuclear antigen for anticancer therapy. *J. Cell. Biochem.* **2022**, 1091.
(69) Hameed, A.; Shafiq, Z.; Yaqub, M.; Hussain, M.; Ahmad, H. B.; Tahirb, M. N.; Naseer, M. M., *Robustness of a thioamide {ÁÁÁH−N−CQS} 2 synthon: synthesis and the effect of substituents on the formation of layered to cage-like supramolecular networks in coumarin−thiosemicarbazone hybrids1*. 2015.
(70) McConkey, B. J.; Sobolev, V.; Edelman, M. The performance of current methods in ligand−protein docking. *Curr. Sci.* **2002**, 845−856.
(71) Meng, X.-Y.; Zhang, H.-X.; Mezei, M.; Cui, M. Molecular docking: a powerful approach for structure-based drug discovery. *Curr. Comput.-Aided Drug Des.* **2011**, *7*, 146−157.
(72) Wang, G.; Zhu, W. Molecular docking for drug discovery and development: a widely used approach but far from perfect. *Future Sci.* **2016**, *8*, 1707−1710.
(73) Iqbal, S.; Saleem, M.; Azim, M. K.; Taha, M.; Salar, U.; Khan, K. M.; Perveen, S.; Choudhary, M. I. Carbohydrazones as new class of carbonic anhydrase inhibitors: Synthesis, kinetics, and ligand docking studies. *Bioorg. Chem.* **2017**, *72*, 89−101.
(74) Karak, S.; Nag, G.; De, B. Metabolic profile and β-glucuronidase inhibitory property of three species of Swertia. *Rev. Bras. Farmacogn.* **2017**, *27*, 105−111.
(75) Abagyan, R.; Totrov, M. Biased probability Monte Carlo conformational searches and electrostatic calculations for peptides and proteins. *J. Mol. Biol.* **1994**, *235*, 983−1002.

https://doi.org/10.1021/acsomega.2c03528
ACS Omega 2022, 7, 28605−28617

(76) Sjöblom, B.; Polentarutti, M.; Djinović-Carugo, K. Structural study of X-ray induced activation of carbonic anhydrase. *Proc. Natl. Acad. Sci.* **2009**, *106*, 10609−10613.
(77) Wallace, B. D.; Roberts, A. B.; Pollet, R. M.; Ingle, J. D.; Biernat, K. A.; Pellock, S. J.; Venkatesh, M. K.; Guthrie, L.; O'Neal, S. K.; Robinson, S. J.; Dollinger, M.; Figueroa, E.; McShane, S. R.; Cohen, R. D.; Jin, J.; Frye, S. V.; Zamboni, W. C.; Pepe-Ranney, C.; Mani, S.; Kelly, L.; Redinbo, M. R. Structure and inhibition of microbiome β-glucuronidases essential to the alleviation of cancer drug toxicity. *Chem. Biol.* **2015**, *22*, 1238−1249.

https://doi.org/10.1021/acsomega.2c03528
ACS Omega 2022, 7, 28605−28617